Dynamic Instabilities and Pattern Formation in Diffusive Epidemic Spread ⋆

Aman Kumar Singh * **Grace Miller** ** **Manish Kumar** *** **Subramanian Ramakrishnan** ****

* *School of Advanced Sciences, Vellore Institute of Technology, Tamilnadu-632014, India (e-mail: aman.singh@vit.ac.in).*
** *Department of Mechanical and Aerospace Engineering University of Dayton, Dayton OH, USA (e-mail: millerg15@udayton.edu)*
*** *Department of Mechanical and Materials Engineering, University of Cincinnati, Cincinnati OH, USA, (e-mail: manish.kumar@uc.edu)*
**** *Department of Mechanical and Aerospace Engineering, University of Dayton, Dayton OH, USA (e-mail: sramakrishnan1@udayton.edu)*

Abstract: The COVID-19 pandemic has refocused research on mathematical modeling and analysis of epidemic dynamics. We analytically investigate a partial differential equation (PDE) based, compartmental model of spatiotemporal epidemic spread, marked by strongly nonlinear infection forces representing the infection transmission mechanism. Employing higher-order perturbation analysis and computing the local Lyapunov exponent, we observe the emergence of dynamic instabilities induced by stochastic environmental forces driving the epidemic spread. Notably, the instabilities are uncovered using third-order perturbations whilst they are not observed under second-order perturbations. Moreover, the onset of instability is more likely with increasing noise strength of the stochastic environmental forces.

Keywords: Epidemic modeling, partial differential equations, instabilities, perturbation theory, stochastic analysis, noise.

1. INTRODUCTION

The COVID-19 pandemic underscores the need for accurate predictive mathematical models of epidemic spread that can also help design control interventions for spread mitigation. A fruitful modeling approach is to treat an epidemic as a *stochastic dynamic system* [Allen (2017)], the *spatiotemporal* evolution of which is dictated by a system of coupled partial differential equations (PDE) of the reaction-diffusion type. In recent work, two of the co-authors (S.R. and M.K.) and their colleagues analyzed and validated such a PDE model using COVID-19 spread data from Ohio, US [Majid et al. (2022, 2021)]. Here we investigate the dynamic instabilities of this PDE model using a *higher-order* perturbative approach. The motivation is two-fold:(1) dynamic instabilities can be a powerful tool in characterizing abrupt and drastic changes in epidemic spread patterns (e.g. super spreading events), (2) there exist deep results on such instabilities and pattern formation in standard reaction-diffusion systems, going back to the Turing instability which we briefly discuss now.

In 1952, Alan Turing discovered that a homogeneous steady state of a reaction-diffusion system can become unstable due to the disparity of diffusion coefficients of the two reacting species involved [Turing (1952); Painter et al. (1999); Meinhardt (1982)]. Remarkably, experimental evidence for such instability was reported in the 1990s [Murray (1993)] and has spurred further research ever since [Riaz et al. (2007); Landge et al. (2020)]. A key point here is that Turing's stability analysis is hinged on the *linearization* of the dynamics near the steady state. As such, despite its spectacular success in linear reaction-diffusion PDE, the Turing approach is silent in the case of nonlinear systems. However, it has inspired *higher-order* perturbative approaches to elucidate the role of nonlinearity in determining the instability conditions leading to pattern formation in stochastic systems [Riaz et al. (2007); Dutta et al. (2005); Riaz et al. (2005)].

In this paper, we report on the emergence of instabilities and pattern formation in a stochastic version of the previously mentioned PDE model of epidemic spread, studied using higher-order perturbative analysis. A central question - essential to justifying our approach - is the mechanism by which nonlinearities enter the epidemic PDE model. While the details are provided later in the paper, here we present the key idea. The PDE model is a compartmental model of epidemic spread; a population is partitioned into disjoint subsets of Susceptible (S), Infected (I), and Recovered (R) individuals and an epidemic evolves as the I compartment gains individuals due to interaction with the S compartment. Mathematically, this process of conversion is characterized by the *infection force*. Based on empirical evidence and factors such as human behavior patterns and saturation effects, the infection force is often best represented by strongly

⋆ S.R. would like to acknowledge partial support for this work from NSF Grant No: CMMI 2140405 and M.K. would like to acknowledge partial support for this work from NSF Grant No: CMMI 2140420

nonlinear functions [Capasso and Serio (1978); Xiao and Ruan (2007); Rohith and Devika (2020)]. Consequently, the epidemic PDE model becomes nonlinear. Moreover, we consider the PDE for the infected population density (I) to also be forced by a white noise term. Thus, external uncertainties - entirely expected to influence the spread of infection - are taken into account in our stability analysis.

The rest of the paper is set as follows. The analytic framework and the research methodology are presented in Section 2. The results are presented in Section 3. The paper concludes in Section 4 with a discussion of the results and concluding remarks.

2. ANALYTIC FRAMEWORK AND METHODOLOGY:

In the compartmental models that provide the basis for this work, the complete system of reaction-diffusion type PDEs representing epidemic spread dynamics comprises of four coupled PDEs - one each for the Susceptible (S), Latent (L), Infected (I), and Recovered (R) population densities corresponding to the four respective compartments [Li and Zou (2009); Yang et al. (2022); Bjørnstad et al. (2020)]. However, re-infections lie outside the scope of the present analysis, and since L does not contribute directly to the infection force in the model, the dynamics of the reduced system of coupled PDEs for S and I may be fruitfully analyzed for stability. Hence we focus on the reduced system for our analysis.

Next, we turn to the rate of infection. In basic models without saturation, the rate of infection is defined as $\beta(I) = \beta_0 I$, where β_0 represents the per capita contact, and I is the infected population density. However, upon taking saturation into account, the rate of infection $\beta(I)$ can be modeled as [Xiao and Ruan (2007)]

$$\beta(I) = \frac{\beta_0 I}{1 + \alpha I^2}, \tag{1}$$

where the term $1 + \alpha I^2$ represents the inhibition effect, usually interpreted as the 'psychological' effect. This psychological effect is usually a consequence of aggressive governmental measures - represented by α - such as isolation, quarantine, restriction of public movement, aggressive sanitation, and so on [Gumel et al. (2004)]. For lower values of infection, a population might take an epidemic less seriously, and this could increase the rate of infection rapidly. However, as more and more people around get infected, the population is increasingly likely to respond positively to protection measures. The term 'psychological' effect connotes the behavioral change of the susceptible public when an epidemic is perceived to be spreading rapidly. The behavioral change could be manifest in the increased acceptance of protective measures such as social distancing, sanitation, self-isolation, and masking. This behavior is represented as a non-monotonous function, $\beta(I)$, as presented in Eq. (1). In this work, α is a positive constant that represents the rate of saturation.

2.1 Model:

Adopting a nonlinear infection force with saturation effects (Rohith and Devika (2020)), the reduced system of coupled PDEs for S and I may be obtained as:

$$\frac{\partial S\,(x,y,t)}{\partial t} = b - dS - \frac{\beta_0\ SI}{1+\alpha I^2} + D_1\nabla^2 S, \tag{2a}$$

$$\frac{\partial I\,(x,y,t)}{\partial t} = \frac{\beta_0\ SI}{1+\alpha I^2} - \gamma I + D_2\nabla^2 I + \xi\,(t,x,y)\,, \tag{2b}$$

where b, the birth rate, d, and γ the death rates, D_1, and D_2 are the diffusion coefficients for the population densities S, and I respectively, ∇^2 is the Laplacian, and $\xi(t,x,y)$ is spatiotemporal Gaussian white noise with

$$\langle \xi\,(t_1,x_1,y_1)\,\xi\,(t_2,x_2,y_2)\rangle = 2D_I\delta\,(x_1-x_2)\,\delta\,(y_1-y_2)\,\delta\,(t_1-t_2)\,. \tag{3}$$

Let (S_0, I_0) be the homogeneous steady state of the system described by Equations (2). The quantities S_0, and I_0 are obtained by setting the right-hand side of Eq. 2 to zero, along with vanishing diffusion and noise terms. Thus (S_0, I_0) simultaneously satisfies:

$$b - dS_0 - \frac{\beta_0\ S_0 I_0}{1+\alpha I_0^2} = 0, \tag{4a}$$

$$\frac{\beta_0\ S_0 I_0}{1+\alpha I_0^2} - \gamma I_0 = 0. \tag{4b}$$

The acceptable nontrivial solution of Eq. (4) is obtained as

$$S_0 = \frac{\gamma}{\beta_0} + \frac{\alpha\gamma}{\beta_0} I_0^2,$$

$$I_0 = -\frac{-\beta_0}{\alpha d} + \sqrt{\left(\frac{\beta_0}{\alpha d}\right)^2 - 4\left(\frac{1}{\alpha} - \frac{b\beta_0}{\alpha\gamma d}\right)}.$$

For $I_0 > 0$, we must have $b\beta_0 > \gamma d$. Under noise free and diffusion-less condition, the solution (S_0, I_0) is stable. However, it is seen that competing populations, if allowed to diffuse, will self-organize in unique patterns. In other words, pattern formation emerges if diffusion causes instability in the homogeneous steady solution - the phenomenon at the core of the Turing instability. Moreover, as noted previously it may also be possible that diffusion alone cannot be sufficient for instability in the epidemic model. However, diffusing populations may undergo instabilities in the presence of noise of even small intensity. These aspects are investigated in this work.

2.2 Stability and Moments

In order to analyze stability, we perturb the system from its uniform steady solutions, i.e., $S_0 \to S_0 + \delta S$, and $I_0 \to I_0 + \delta I$. However, we go beyond standard linear stability analysis and invoke the Taylor series expansion up to *third order* in the perturbation around (S_0, I_0) in our analysis. We rewrite Eq. (2) in the following form as

$$\frac{\partial S\,(x,y,t)}{\partial t} = F(S,I) + D_1\nabla^2 S, \tag{5a}$$

$$\frac{\partial I\,(x,y,t)}{\partial t} = G(S,I) + D_2\nabla^2 I + \xi\,(t,x,y)\,, \tag{5b}$$

where

$$F(S,I) = b - dS - \frac{\beta_0\ SI}{1+\alpha I^2} \tag{6a}$$

$$G(S,I) = \frac{\beta_0\ SI}{1+\alpha I^2} - \gamma I. \tag{6b}$$

Then in Eq. (2) under substitution $S \to S_0 + \delta S$, and $I \to I_0 + \delta I$ followed by the Taylor expansion around (S_0, I_0), we obtain

$$\frac{\partial \delta S}{\partial t} = F_S\delta S + F_I\delta I + (1/2)\,F_{SS}\delta S^2 + (1/2)\,F_{II}\delta I^2 + F_{SI}\delta S\delta I + (1/6)\,F_{SSS}\delta S^3 + (1/6)\,F_{III}\delta I^3 + (1/2)\,F_{SSI}\delta S^2\delta I + (1/2)\,F_{SII}\delta S\delta I^2 + D_1(\delta S_{xx} + \delta S_{yy}), \quad (7)$$

where $F_S = \frac{\partial F}{\partial S}$ evaluated at point (S_0, I_0). Similarly, we have

$$\frac{\partial \delta I}{\partial t} = G_S\delta S + G_I\delta I + (1/2)\,G_{SS}\delta S^2 + (1/2)\,G_{II}\delta I^2 + G_{SI}\delta S\delta I + (1/6)\,G_{SSS}\delta S^3 + (1/6)\,G_{III}\delta I^3 + (1/2)\,G_{SSI}\delta S^2\delta I + (1/2)\,G_{SII}\delta S\delta I^2 + D_2(\delta I_{xx} + \delta I_{yy}) + \xi(t,x,y). \quad (8)$$

We discretize the system of equations Eqs. (7), and (8) at a lattice site (i, j), and obtain

$$\frac{\partial \delta S_{ij}}{\partial t} = F_S\delta S_{ij} + F_I\delta I_{ij} + (1/2)\,F_{SS}\delta S_{ij}^2 + (1/2)\,F_{II}\delta I_{ij}^2 + F_{SI}\delta S_{ij}\delta I_{ij} + (1/6)\,F_{SSS}\delta S_{ij}^3 + (1/6)\,F_{III}\delta I_{ij}^3 + (1/2)\,F_{SSI}\delta S_{ij}^2\delta I_{ij} + (1/2)\,F_{SII}\delta S_{ij}\delta I_{ij}^2 - k^2 D_1\delta S_{ij}, \quad (9)$$

$$\frac{\partial \delta I_{ij}}{\partial t} = G_S\delta S_{ij} + G_I\delta I_{ij} + (1/2)\,G_{SS}\delta S_{ij}^2 + (1/2)\,G_{II}\delta I_{ij}^2 + G_{SI}\delta S_{ij}\delta I_{ij} + (1/6)\,G_{SSS}\delta S_{ij}^3 + (1/6)\,G_{III}\delta I_{ij}^3 + (1/2)\,G_{SSI}\delta S_{ij}^2\delta I_{ij} + (1/2)\,G_{SII}\delta S_{ij}\delta I_{ij}^2 - k^2 D_2\delta I_{ij}) + \xi_{ij}(t), \quad (10)$$

where we have used $\delta S(x,y,t) = p(t)\cos k_x x \cos k_y y$, $\delta I(x,y,t) = q(t)\cos k_x x \cos k_y y$, and $k^2 = k_x^2 + k_y^2$. Hence $\nabla^2\delta S(x,y,t) = -k^2\delta S(x,y,t)$, and $\nabla^2\delta I(x,y,t) = -k^2\delta I(x,y,t)$ (please see, for instance Riaz et al. (2007). In discrete form, the correlation of ξ is given by

$$\langle \xi(t_1)_{ij}\xi(t_2)_{kl}\rangle = 2C_I\delta_{ik}\delta_{jl}\delta(t_2 - t_1), \quad (11)$$

where $C_I = \frac{D_I}{L_x L_y}$ for a grid size of $L_x \times L_y$. However, we discard the symbol (ij) from now and we shall assume that we are dealing at lattice site (ij), i.e., $\delta S_{ij} \to \delta S$ and it applies to all the variables as well. The statistical averaging of Eqs. (9), and (10) produces

$$\langle\delta S\rangle_t = F_S\langle\delta S\rangle + F_I\langle\delta I\rangle + (1/2)\,F_{SS}\langle\delta S^2\rangle + (1/2)\,F_{II}\langle\delta I^2\rangle + F_{SI}\langle\delta S\delta I\rangle + (1/6)\,F_{SSS}\langle\delta S^3\rangle + (1/6)\,F_{III}\langle\delta I^3\rangle + (1/2)\,F_{SSI}\langle\delta S^2\delta I\rangle + (1/2)\,F_{SII}\langle\delta S\delta I^2\rangle - k^2 D_1\langle\delta S\rangle, \quad (12)$$

and

$$\langle\delta I\rangle_t = G_S\langle\delta S\rangle + G_I\langle\delta I\rangle + (1/2)\,G_{SS}\langle\delta S^2\rangle + (1/2)\,G_{II}\langle\delta I^2\rangle + G_{SI}\langle\delta S\delta I\rangle + (1/6)\,G_{SSS}\langle\delta S^3\rangle + (1/6)\,G_{III}\langle\delta I^3\rangle + (1/2)\,G_{SSI}\langle\delta S^2\delta I\rangle + (1/2)\,G_{SII}\langle\delta S\delta I^2\rangle - k^2 D_2\langle\delta I\rangle. \quad (13)$$

We also see that Eqs. (12), and (13) have higher order moments also, to mention, $\langle\delta S^2\rangle$, $\langle\delta I^2\rangle$, $\langle\delta I\delta S\rangle$, $\langle\delta S^3\rangle$, $\langle\delta I^3\rangle$, $\langle\delta S^2\delta I\rangle$, and $\langle\delta I^2\delta S\rangle$. For the solution of Eqs. (12), and (13), one must have knowledge of evolution of these higher moments. We find the equations of motion for higher moments using Eqs. (7), and (8), for instance, to get the evolution of $\langle\delta S^2\rangle$, we multiply Eq. (7) by $2\delta S$ followed by statistical averaging. Also, we truncate the moments at third order to break the hierarchy. We encounter term like $\langle 2\xi\delta S\rangle$, that we simplify using Novikov's theorem for the Gaussian noise process, i.e.,

$$\langle F(u)\xi\rangle = C_I\langle F(u)F(u')\rangle. \quad (14)$$

In Eqs. (12), and (13), we substitute the values of partial derivatives and obtain

$$\langle\delta S\rangle_t = -\left[k^2 D_1 + d + \frac{\beta_0 I_0}{1+\alpha I_0^2}\right]\langle\delta S\rangle - \frac{\beta_0 S_0(1-\alpha I_0^2)}{(1+\alpha I_0^2)^2}\langle\delta I\rangle + \frac{\alpha\beta_0 S_0 I_0(1-3\alpha I_0^2)}{(1+\alpha I_0^2)^3}\langle\delta I^2\rangle + \frac{\beta_0(1-\alpha I_0^2)}{(1+\alpha I_0^2)^2}\langle\delta S\delta I\rangle + \frac{\alpha\beta_0 I_0(1-3\alpha I_0^2)}{(1+\alpha I_0^2)^3}\langle\delta S\delta I^2\rangle + (1/6)\,\alpha\beta_0 S_0\frac{[3(1-\alpha I_0^4) - 3(3-\alpha I_0^2)]}{(1+\alpha I_0^2)^4}\langle\delta I^3\rangle. \quad (15)$$

$$\langle\delta I\rangle_t = -\left[k^2 D_2 + \gamma - \frac{\beta_0 S_0(1-\alpha I_0^2)}{(1+\alpha I_0^2)^2}\right]\langle\delta I\rangle + \frac{\beta_0 I_0}{(1+\alpha I_0^2)}\langle\delta S\rangle + \frac{\alpha\beta_0 S_0 I_0(3-\alpha I_0^2)}{(1+\alpha I_0^2)^3}\langle\delta I^2\rangle - \frac{\beta_0(1-\alpha I_0^2)}{(1+\alpha I_0^2)^2}\langle\delta S\delta I\rangle - \frac{\alpha\beta_0 I_0(1-3\alpha I_0^2)}{(1+\alpha I_0^2)^3}\langle\delta S\delta I^2\rangle + (1/6)\,\alpha\beta_0 S_0\frac{[3(1-\alpha I_0^4) - 3(3-\alpha I_0^2)]}{(1+\alpha I_0^2)^4}\langle\delta I^3\rangle. \quad (16)$$

The evolution of higher moments is given as

$$\langle\delta S^2\rangle_t = -2\left[k^2 D_1 + d + \frac{\beta_0 I_0}{1+\alpha I_0^2}\right]\langle\delta S^2\rangle - 2\frac{\beta_0 S_0(1-\alpha I_0^2)}{(1+\alpha I_0^2)^2}\langle\delta I\delta S\rangle + 2\frac{\alpha\beta_0 S_0 I_0(1-3\alpha I_0^2)}{(1+\alpha I_0^2)^3}\langle\delta I^2\delta S\rangle - 2\frac{\beta_0(1-\alpha I_0^2)}{(1+\alpha I_0^2)^2}\langle\delta S^2\delta I\rangle. \quad (17)$$

$$\langle\delta I^2\rangle_t = 2C_I\langle\delta I\rangle - 2\left[k^2 D_2 + \gamma - \frac{\beta_0 S_0(1-\alpha I_0^2)}{(1+\alpha I_0^2)^2}\right]\langle\delta I^2\rangle + 2\frac{\beta_0 I_0}{(1+\alpha I_0^2)}\langle\delta S\delta I\rangle + 2\frac{\alpha\beta_0 S_0 I_0(3-\alpha I_0^2)}{(1+\alpha I_0^2)^3}\langle\delta I^3\rangle - 2\frac{\beta_0(1-\alpha I_0^2)}{(1+\alpha I_0^2)^2}\langle\delta S\delta I^2\rangle. \quad (18)$$

$$\langle \delta I \delta S \rangle_t = C_I \langle \delta S \rangle - \Big[k^2(D_1+D_2) + (\gamma + d) + \frac{\beta_0 I_0}{1+\alpha I_0^2} - \frac{\beta_0 S_0 (1-\alpha I_0^2)}{(1+\alpha I_0^2)^2} \Big] \langle \delta I \delta S \rangle + \frac{\alpha \beta_0 S_0 I_0 (3-\alpha I_0^2)}{(1+\alpha I_0^2)^3} \langle \delta I^3 \rangle + \Big[\frac{\alpha \beta_0 S_0 I_0 (3-\alpha I_0^2)}{(1+\alpha I_0^2)^3} - \frac{\beta_0 (1-\alpha I_0^2)}{(1+\alpha I_0^2)^2} \Big] \langle \delta I^2 \delta S \rangle + \frac{\beta_0 I_0}{(1+\alpha I_0^2)} \langle \delta S^2 \rangle - \frac{\beta_0 (1-\alpha I_0^2)}{(1+\alpha I_0^2)^2} \langle \delta S^2 \delta I \rangle. \quad (19)$$

$$\langle \delta I^3 \rangle_t = -3 \Big[-2C_I + k^2 D_2 + \gamma - \frac{\beta_0 S_0 (1-\alpha I_0^2)}{(1+\alpha I_0^2)^2} \Big] \langle \delta I^3 \rangle + 3 \frac{\beta_0 I_0}{(1+\alpha I_0^2)} \langle \delta S \delta I^2 \rangle. \quad (20)$$

$$\langle \delta I \delta S^2 \rangle_t = - \Big[k^2(D_2+2D_1) + (\gamma + 2d) + \frac{2\beta_0 I_0}{1+\alpha I_0^2} - \frac{\beta_0 S_0 (1-\alpha I_0^2)}{(1+\alpha I_0^2)^2} \Big] \langle \delta I \delta S^2 \rangle + \Big[2C_I + \frac{\beta_0 I_0}{1+\alpha I_0^2} \Big] \langle \delta S^3 \rangle - \frac{2\beta_0 S_0 (1-\alpha I_0^2)}{(1+\alpha I_0^2)^2} \langle \delta I^2 \delta S \rangle. \quad (21)$$

$$\langle \delta S^3 \rangle_t = -3 \Big[k^2 D_1 + d + \frac{\beta_0 I_0}{1+\alpha I_0^2} \Big] \langle \delta S^3 \rangle - 3 \frac{\beta_0 S_0 (1-\alpha I_0^2)}{(1+\alpha I_0^2)^2} \langle \delta I \delta S^2 \rangle. \quad (22)$$

$$\langle \delta I^2 \delta S \rangle_t = 2C_I \langle \delta I \delta S \rangle - \Big[k^2(D_1+2D_2) + (d+2\gamma) + \frac{\beta_0 S_0}{1+\alpha I_0^2} - \frac{2\beta_0 S_0 (1-\alpha I_0^2)}{(1+\alpha I_0^2)^2} \Big] \langle \delta I^2 \delta S \rangle + 2 \frac{\beta_0 I_0}{1+\alpha I_0^2} \langle \delta I \delta S^2 \rangle - \frac{\beta_0 S_0 (1-\alpha I_0^2)}{(1+\alpha I_0^2)^2} \langle \delta I^3 \rangle. \quad (23)$$

We can also write these coupled linear equations for moments are summarized in the following form as:

$$\dot{X} = AX, \quad (24)$$

where $X = (x_1, x_2, x_3, x_4, x_5, x_6, x_7, x_8, x_9)^T$, and A is a 9×9 matrix. The components x_i are given as $x_1 = \langle \delta S \rangle$, $x_2 = \langle \delta I \rangle$, $x_3 = \langle \delta S^2 \rangle$, $x_4 = \langle \delta I^2 \rangle$, $x_5 = \langle \delta I \delta S \rangle$, $x_6 = \langle \delta S^3 \rangle$, $x_7 = \langle \delta I^3 \rangle$, $x_8 = \langle \delta S^2 \delta I \rangle$, $x_9 = \langle \delta I^2 \delta S \rangle$. The matrix A is obtained as

$$A = \begin{bmatrix} a_1 & a_2 & a_3 & a_4 & a_5 & a_6 & a_7 & a_8 & a_9 \\ b_1 & b_2 & 0 & a_4 & a_5 & 0 & a_7 & 0 & -a_9 \\ 0 & 0 & 2a_1 & 0 & 2a_2 & 0 & 0 & -2a_5 & 2a_4 \\ 0 & 2C_I & 0 & 2b_2 & 2b_1 & 0 & 2a_4 & 0 & -2a_5 \\ C_I & 0 & b_1 & 0 & s_1 & 0 & a_4 & -a_5 & s_2 \\ 0 & 0 & 0 & 0 & 0 & 3a_1 & 0 & 3a_2 & 0 \\ 0 & 0 & 0 & 0 & 0 & 0 & s_3 & 0 & 3b_1 \\ 0 & 0 & 0 & 0 & 0 & s_4 & 0 & s_5 & 2a_2 \\ 0 & 0 & 0 & 0 & 2C_I & 0 & a_2 & 2b_1 & s_6 \end{bmatrix}, \quad (25)$$

where $s_1 = a_1 + b_2$, $s_2 = a_4 - a_5$, $s_3 = 3b_2 + 6C_I$, $s_4 = b_1 + 2C_I$, $s_5 = b_2 + 2a_1$, $s_6 = a_1 + 2b_2$ and other parameters are defined as:

$$a_1 = -\left[k^2 D_1 + d + \frac{\beta_0 I_0}{1+\alpha I_0^2} \right], \quad (26a)$$

$$a_2 = -\frac{\beta_0 S_0 \left(1-\alpha I_0^2\right)}{\left(1+\alpha I_0^2\right)^2}, \quad (26b)$$

$$a_3 = 0, \quad (26c)$$

$$a_4 = \frac{\alpha \beta_0 S_0 I_0 \left(1-3\alpha I_0^2\right)}{\left(1+\alpha I_0^2\right)^3}, \quad (26d)$$

$$a_5 = \frac{\beta_0 \left(1-\alpha I_0^2\right)}{\left(1+\alpha I_0^2\right)^2}, \quad (26e)$$

$$a_6 = 0, \quad (26f)$$

$$a_7 = \frac{1}{6} \frac{\alpha \beta_0 S_0 \left[3\left(1-\alpha I_0^4\right) - 3\left(3-\alpha I_0^2\right)\right]}{1+\alpha I_0^2}, \quad (26g)$$

$$a_8 = 0, \quad (26h)$$

$$a_9 = \frac{\alpha \beta_0 I_0 \left(1-3\alpha I_0^2\right)}{\left(1+\alpha I_0^2\right)^3}, \quad (26i)$$

$$b_1 = \frac{\beta_0 I_0}{1+\alpha I_0^2}, \quad (26j)$$

$$b_2 = -\left[k^2 D_2 + \gamma - \frac{\beta_0 S_0 \left(1-\alpha I_0^2\right)}{\left(1+\alpha I_0^2\right)^2} \right]. \quad (26k)$$

3. RESULTS

The onset of instability is characterized by the emergence of a positive eigenvalue (local Lyapunov exponent) of the matrix A. In order to get a range of values of k over which instability persists, the dispersion relation $Re\ \lambda(k^2)$ is plotted with k^2 for three different values of noise strength (C_I) in Fig. 1 for second order Taylor expansion. Irrespective of the noise level, we do not find any instability as λ is negative and the uniform solution (S_0, I_0) is stable. We also explore the range of saturation parameter α but we have not found any instability [see, Fig. (2)]. With the third order stability analysis, in deterministic case, we do not see the instability [see, Fig. (3), dashed-dot curve.]. However, under the influence of noise, we see that $\lambda > 0$ in a certain range of k. Furthermore, this range of k expands with increasing values of noise strength (C_I) [see, Fig. (3), solid curve and curve marked with dot]. The range of saturation parameter (α) for instability can be obtained from Fig. (4). Thus, these preliminary results suggest the onset of instabilities (and hence new pattern formations in spatiotemporal epidemic spread) for the specified range of k values, in the case of the nonlinear infection force with saturation effects analyzed. Ongoing investigations are currently focused on comparing these results with the case of the infection force without saturation effects. Finally, these results provide the basis for further stability analyses of the PDE epidemic model.

4. DISCUSSION AND CONCLUDING REMARKS

For the nonlinear infection force considered (that accounts for saturation effects), a second-order perturbation analysis did not yield instabilities, both in the deterministic and

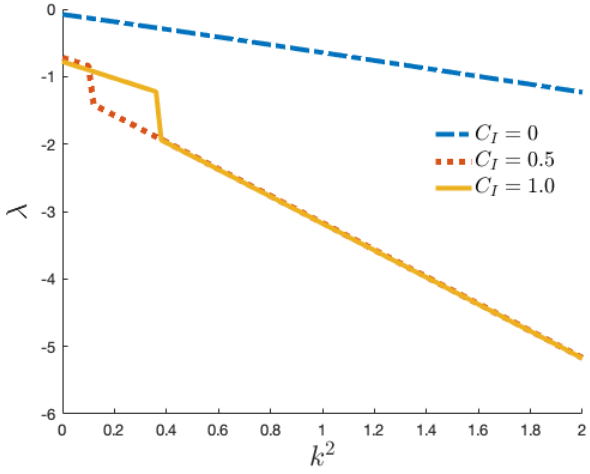

Fig. 1. The variation of largest local Lyapunov exponent (λ) with wave number k for second order. The values other of parameters are: $d = 0.5$, $\gamma = 0.4$, $\alpha = 0.4$, $\beta_0 = 0.8$, $b = 0.3$, $D_1 = 1$, and $D_2 = 0.6$

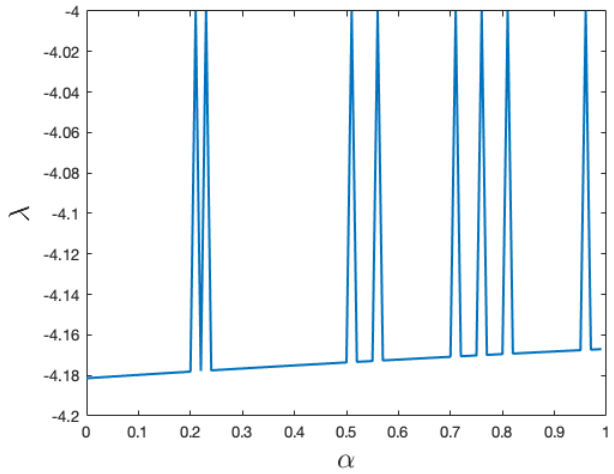

Fig. 2. The variation of largest local Lyapunov exponent (λ) with the saturation parameter α for second order. The values other of parameters are: $d = 0.5$, $\gamma = 0.4$, $k^2 = 1.5$, $\beta_0 = 0.8$, $b = 0.3$, $D_1 = 1$, $C_I = 0.5$ and $D_2 = 0.6$

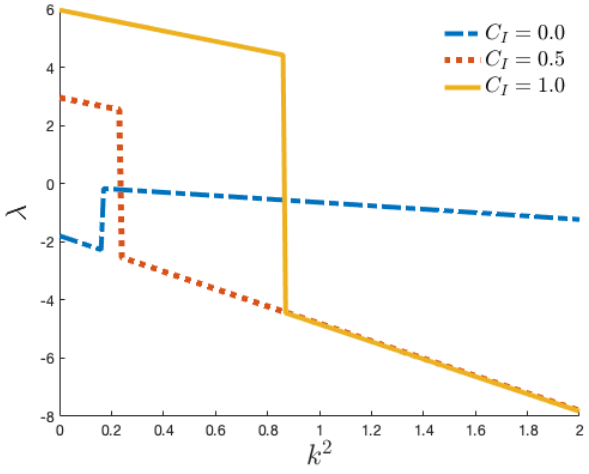

Fig. 3. The variation of largest local Lyapunov exponent (λ) with wave number k for third order. The values other of parameters are: $d = 0.5$, $\gamma = 0.4$, $\alpha = 0.4$, $\beta_0 = 0.8$, $b = 0.3$, $D_1 = 1$, and $D_2 = 0.6$

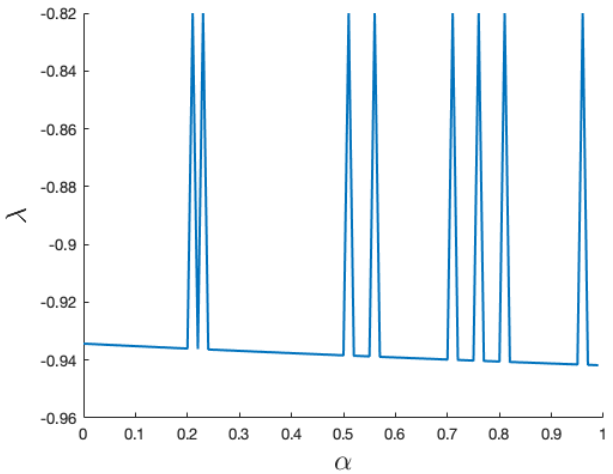

Fig. 4. The variation of largest local Lyapunov exponent (λ) with the saturation parameter α for third order. The values other of parameters are: $d = 0.5$, $\gamma = 0.4$, $k^2 = 1.5$, $\beta_0 = 0.8$, $b = 0.3$, $D_1 = 1$, $C_I = 0.5$ and $D_2 = 0.6$

stochastic cases. Moreover, this absence of instabilities persisted over a range of noise strengths as well as values of the saturation parameter. However, a third-order perturbation led to remarkably different conclusions. While no instabilities were observed for deterministic dynamics in this case as well, instabilities were observed for a certain range of values of the dispersion parameter k in the stochastic case. Furthermore, this range of values of k expanded further with increasing noise strength driving the PDE epidemic model. That the third-order perturbation uncovered the instability while the second-order perturbation did not is the first main result of this work. The expansion in the range of k values (supporting the onset of instabilities) with increasing noise intensities is our second main result. In light of these results, investigating the emergence of instabilities for other, strongly nonlinear infection forces is a subject of our ongoing research. In addition, we expect these results to be significant in the context of other nonlinear dynamic problems represented by similar PDE systems. We conclude with the hope that the results presented in this paper open multiple pathways for further research.

REFERENCES

Allen, L.J. (2017). A primer on stochastic epidemic models: Formulation, numerical simulation, and analysis. *Infectious Disease Modelling*, 2(2), 128–142.

Bjørnstad, O.N., Shea, K., Krzywinski, M., and Altman, N. (2020). The SEIRS model for infectious disease dynamics. *Nature Methods*, 17, 557–558.

Capasso, V. and Serio, G. (1978). A generalization of the Kermack-McKendrick deterministic epidemic model. *Mathematical Biosciences*, 42(1), 43–61.

Dutta, S., Riaz, S.S., and Ray, D.S. (2005). Noise-induced instability: an approach based on higher-order moments. *Physical Review E*, 71(3), 036216.

Gumel, A.B., Ruan, S., Day, T., Watmough, J., Brauer, F., van den Driessche, P., Gabrielson, D., Bowman, C., Alexander, M.E., Ardal, S., Wu, J., and Sahai, B.M. (2004). Modelling strategies for controlling sars outbreaks. *Proceedings of the Royal Society of London. Series B: Biological Sciences*, 271(1554), 2223–2232.

Landge, A.N., Jordan, B.M., Diego, X., and Müller, P. (2020). Pattern formation mechanisms of self-organizing reaction-diffusion systems. *Developmental Biology*, 460(1), 2–11. Systems Biology of Pattern Formation.

Li, J. and Zou, X. (2009). Modeling spatial spread of infectious diseases with a fixed latent period in a spatially continuous domain. *Bull. Math. Biol.*, 71, 2048–2079.

Majid, F., Deshpande, A.M., Ramakrishnan, S., Ehrlich, S., and Kumar, M. (2021). Analysis of epidemic spread dynamics using a pde model and covid-19 data from hamilton county oh usa. *IFAC-PapersOnLine*, 54(20), 322–327.

Majid, F., Gray, M., Deshpande, A.M., Ramakrishnan, S., Kumar, M., and Ehrlich, S. (2022). Non-pharmaceutical interventions as controls to mitigate the spread of epidemics: An analysis using a spatiotemporal pde model and covid–19 data. *ISA Transactions*, 124, 215–224.

Meinhardt, H. (1982). Models of biological pattern formation. *Academic press, London*, 118.

Murray, J. (1993). Mathematical biology. *Springer-Verlag, Berlin*.

Painter, K.J., Maini, P.K., and Othmer, H.G. (1999). Stripe formation in juvenile pomacanthus explained by a generalized turing mechanism with chemotaxis. *Proceedings of the National Academy of Sciences*, 96(10), 5549–5554.

Riaz, S., Kar, S., and Ray, D. (2005). Pattern formation induced by additive noise: a moment-based analysis. *The European Physical Journal B-Condensed Matter and Complex Systems*, 47, 255–263.

Riaz, S.S., Sharma, R., Bhattacharyya, S.P., and Ray, D.S. (2007). Instability and pattern formation in reaction-diffusion systems: A higher order analysis. *The Journal of Chemical Physics*, 127(6), 064503.

Rohith, G. and Devika, K.B. (2020). Dynamics and control of covid-19 pandemic with nonlinear incidence rates. *Nonlinear Dyn*, 101(6), 2013–2026.

Turing, A.M. (1952). The chemical basis of morphogenesis. *Philosophical Transactions of the Royal Society of London. Series B, Biological Sciences*, 237(641), 37–72.

Xiao, D. and Ruan, S. (2007). Global analysis of an epidemic model with nonmonotone incidence rate. *Mathematical Biosciences*, 208(2), 419–429.

Yang, H., Wang, Y., Kundu, S., Song, Z., and Zhang, Z. (2022). Dynamics of an SIR epidemic model incorporating time delay and convex incidence rate. *Results in Physics*, 32, 105025.